Directed evolution of gene-shuffled IFN-α molecules with activity profiles tailored for treatment of chronic viral diseases

Amy D. Brideau-Andersen*, Xiaojian Huang*, Siu-Chi Chang Sun*, Teddy T. Chen*, Diane Stark*, Ian J. Sas*, Linda Zadik*†, Glenn N. Dawes*, Douglas R. Guptill*, Robert McCord*, Sridhar Govindarajan*, Ajoy Roy*, Shumin Yang*, Judy Gao*, Yong Hong Chen*, Niels Jørgen Ø. Skartved‡, Annette K. Pedersen‡, David Lin*, Christopher P. Locher*, Indrani Rebbapragada*, Anne Dam Jensen‡, Steven H. Bass*, Torben L. Straight Nissen*, Sridhar Viswanathan*, Graham R. Foster§, Julian A. Symons¶, and Phillip A. Patten*†∥

*Maxygen, Incorporated, 515 Galveston Drive, Redwood City, CA 94063; ‡Maxygen, Anpartsselskab, Agern Alle 1, DK-2970 Hoersholm, Denmark; ¶Roche Palo Alto LLC, 3431 Hillview Avenue, Palo Alto, CA 94304; and §Queen Mary's School of Medicine and Dentistry, Institute of Cell and Molecular Science, The Royal London Hospital, 4 Newark Street, London E1 2AT, England

Edited by Peter G. Schultz, The Scripps Research Institute, La Jolla, CA, and approved March 26, 2007 (received for review November 4, 2006)

Type I IFNs are unusually pleiotropic cytokines that bind to a single heterodimeric receptor and have potent antiviral, antiproliferative, and immune modulatory activities. The diverse effects of the type I IFNs are of differential therapeutic importance; in cancer therapy, an enhanced antiproliferative effect may be beneficial, whereas in the therapy of viral infections (such as hepatitis B and hepatitis C), the antiproliferative effects lead to dose limiting bone marrow suppression. Studies have shown that various members of the natural IFN-α family and engineered variants, such as IFN-con1, vary in the ratios between various IFN-mediated cellular activities. We used DNA shuffling to explore and confirm the hypothesis that one could simultaneously increase the antiviral and Th1-inducing activity and decrease the antiproliferative activity. We report IFN-α hybrids wherein the ratio of antiviral:antiproliferative and Th1-inducing: antiproliferative potencies are markedly increased with respect to IFN-con1 (75- and 80-fold, respectively). A four-residue motif that overlaps with the IFNAR1 binding site and is derived by cross breeding with a pseudo-gene contributes significantly to this phenotype. These IFN-αs have an activity profile that may result in an improved therapeutic index and, consequently, better clinical efficacy for the treatment of chronic viral diseases such as hepatitis B virus, human papilloma virus, HIV, or chronic hepatitis C.

evolved | Hepatitis C

T he type I IFNs comprise a family of four helix bundle cytokines encoded by 13 nonallelic IFN-α subtypes, IFN-β, IFN-ε, IFN-κ, IFN-δ, IFN-τ, IFN-ω, and limitin, a recently discovered orthologue found only in mice (1). Although all type I IFNs are recognized by a single shared receptor comprised of two transmembrane subunits, IFNAR-1 and IFNAR-2, these cytokines have an unusually pleiotropic activity profile, including antiproliferative, antiviral, and immunomodulatory activities (1) and consequently this family of cytokines has found clinical application in cancer, chronic viral diseases, and autoimmune diseases (1–3).

Previous studies performed with natural and hybrid human IFNs show significant variation in the ratios of various IFN-mediated activities including antiviral, antiproliferative, natural killer stimulatory, T cell stimulatory, T cell motility, and proliferation of primary B cells (1–3). These studies strongly suggest that there is in principle significant potential to modulate the ratios of the IFN-mediated activities. However, given our incomplete knowledge of the relationship between variation in IFN primary structure, receptor binding and downstream signaling, our ability to engineer the ratios of IFN-mediated activities is in its infancy.

DNA shuffling is a general approach to genetic engineering that exploits natural diversity in gene families and has been used to evolve variants of enzymes, cytokines, antibodies, insect toxins, and viruses (4). Because this method can be applied by using any arbitrary biological readout and requires no structure-function model, we reasoned that this approach would be well suited to testing hypotheses regarding which IFN-mediated activities can be dissected one from another. In this study, we specifically reasoned that for treatment of chronic viral infections (such as HCV, HBV, or HIV) it would be desirable to have increased antiviral activity while minimizing antiproliferative potency, an activity of the drug that may lead to dose limiting side effects such as neutropenia and thrombocytopenia (5). In addition to the direct antiviral activity of IFNs, it has become increasingly clear in model systems (6) and in clinical studies (7, 8) that induction of a robust Th1 response is essential for clearing chronic viral infections. We therefore sought in this study to evolve variants with both increased antiviral and Th1-inducing potency without concomitant increases in antiproliferative potency, using DNA shuffling. Here, we report fifteen evolved members of the IFN-α family that have greater antiviral potency and Th1 inducing activity yet decreased antiproliferative activity relative to IFN-con1, the most potent antiviral type I IFN previously reported.

Results

Library Screening. Three gene-shuffled libraries were screened in a high-throughput screening format for Th1 inducing and antiproliferative activity on Daudi cells [supporting information (SI) Fig. 5]. Those variants that displayed a Th1:antiproliferative activity ratio that was equivalent to or greater than IFN-α8, the most potent wild type IFN-α in the Th1 assay (X.H., G.R.F. data not shown), were subjected to secondary and tertiary rounds of quantitative screening in the Th1 differentiation, Daudi antiproliferation, and several antiviral assays (Table 1 and SI Tables 3–5). The most potent variants in the Th1 differentiation assay all came from library BC9, a gene-shuffled library derived from gene shuffling of degenerate PCR products containing the entire human IFN-α gene family (9).

BIOCHEMISTRY

Table 1. Summary of the relative potencies of the shuffled IFN-α compounds compared with IFN-con1 and IFN-α2b in the Daudi-tritiated thymidine uptake assay

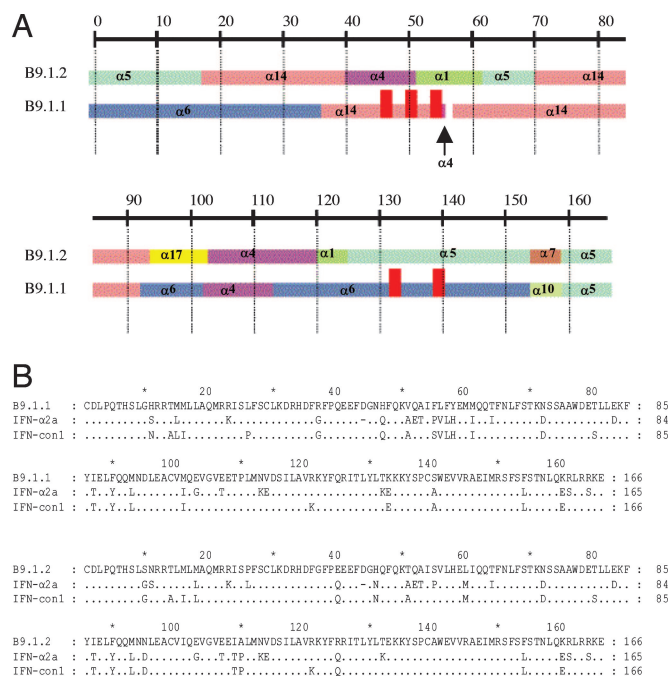| Sample	Mean log EC_{50}	SD	n	Mean EC_{50}, ng/ml	Fold over IFN-α2b	Fold over IFN-con1	Sample vs. IFN-con1, P value
IFN-con1	−2.38	0.412	5	0.00418	1.1	1.0	—
IFN-α2b	−2.35	0.289	8	0.00442	1.0	0.95	0.815
B9X17	−2.30	0.048	3	0.00502	0.88	0.83	0.544
B9.1.2	−2.21	0.286	2	0.00615	0.72	0.68	0.265
B9X23 *	−2.08	0.409	4	0.00832	0.53	0.50	0.0155
B9X22 *	−2.07	0.156	5	0.00848	0.52	0.49	0.00876
B9X18 *	−2.02	0.547	4	0.00958	0.46	0.44	0.00402
B9X25 *	−2.00	0.267	9	0.00991	0.45	0.42	0.000428
B9X14 *	−1.98	0.210	10	0.0105	0.42	0.40	0.000160
B9X24 *	−1.83	0.372	3	0.0149	0.30	0.28	<0.0001
B9X28 *	−1.76	0.411	3	0.0172	0.26	0.24	<0.0001
B9X26 *	−1.70	0.317	3	0.0200	0.22	0.21	<0.0001
B9X16 *	−1.65	0.027	3	0.0223	0.20	0.19	<0.0001
B9X15 *	−1.37	0.215	3	0.0424	0.10	0.10	<0.0001
B9X27 *	−1.24	0.350	5	0.0573	0.077	0.073	<0.0001
B9X12 *	−1.16	0.377	3	0.0696	0.064	0.060	<0.0001

The samples are listed in order of decreasing potency. Fold improvements were calculated as a ratio of mean EC_{50} (ng/ml) values relative to IFN-con1 and IFN-α2b. The mean log EC_{50} values of those interferon samples marked with an asterisk are significantly different at the 95% confidence level from the mean log EC_{50} value of IFN-con1 in the Th1 assay based on a two-way ANOVA and Fisher's least significant difference post hoc test (α = 0.05). The Hill slopes and SDs are: IFN-α2b 0.85 (0.22), IFN-con1 0.83 (0.15), B9X14 0.82 (0.21), B9X25 0.73 (0.10). The dash indicates not applicable.

Among several variants having greater potency than IFN-α8 in the Th1 assay, B9.1.1 and B9.1.2 stood out as having a uniquely high ratio of Th1 and antiviral to antiproliferative activity, and these two variants were chosen for further diversification.

Construction of the B9X Series. The sequence of B9.1.2 is a chimera of eight wild type IFN-α parents (Fig. 1) with no point mutations, whereas B9.1.1 has seven amino acids (47H, 51V, 55F, 56L, 57F, 133K, and 140S) that are derived from a pseudogene within the tandemly duplicated set of IFN-α genes on chromosome 9 (10) and
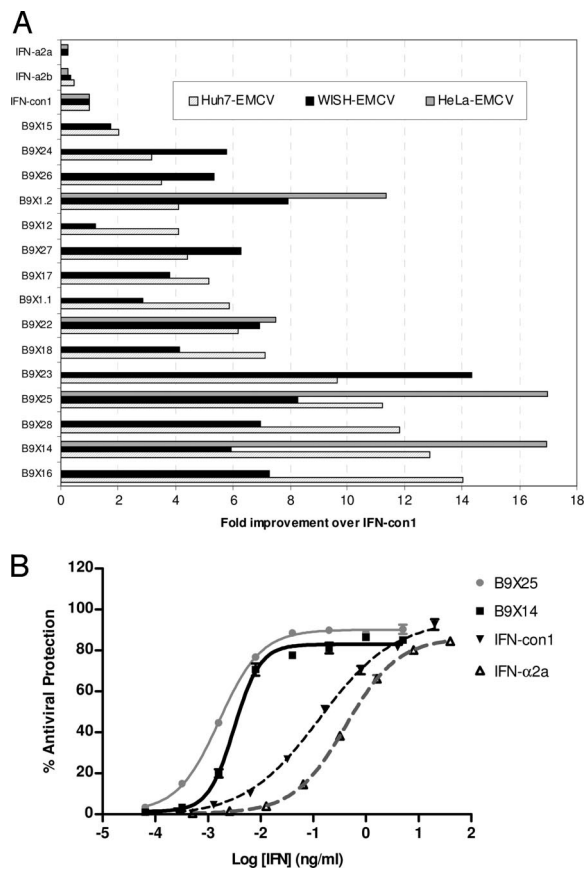
one point mutation (H58Y; SI Fig. 6). This pseudogene has a frame shift in codon 40, which is upstream of the codons that have been incorporated into B9.1.1 and thus the sequences corresponding pseudogene derived residues are not expressed in the context of an IFN-α sequence. Because six of these seven pseudogene-derived residues constitute substitutions not present in any native IFN-α protein (SI Fig. 6) and the H58Y mutation results in a residue present only in IFN-τ (1), we sought to explore the functionality of these residues by permuting them with the corresponding sequences in B9.1.2. This exercise yielded the "B9X" series of shuffled IFN molecules (SI Fig. 7).

Functional Characterization of the B9X Series. We characterized the B9X series in detail to quantitatively rank them with respect to antiviral, antiproliferative-and Th1-inducing activities. Commercial preparations of IFN-con1, human IFN-α2a, and human IFN-α2b were included as reference compounds. We chose the inhibition of replication of encephalomyocarditis virus (EMCV) in the human cell lines Huh7 (hepatoma-derived), HeLa (cervical carcinoma-derived), and WISH (amniotic tissue-derived) as the primary viral protection assays to assess general antiviral potency of our shuffled IFN-α molecules (11).

All shuffled IFN-α molecules tested were significantly more potent than both IFN-con1 and IFN-α2b in the Huh7 EMCV antiviral assay ($P < 0.05$; Fig. 2A and SI Table 3). Similarly, all 15 shuffled IFN-α compounds displayed increased potency over IFN-con1, IFN-α2a, and IFN-α2b in the WISH EMCV antiviral assay (Fig. 2A and SI Table 4). The increased antiviral potency of a subset of these variants (B9.1.2, B9X14, B9X22 and B9X25) over IFN-con1 and IFN-α2b was also confirmed in a HeLa EMCV based antiviral assay (Fig. 2 A and B and SI Table 5). B9X14, one of the most potent variants in all three antiviral assays, is 17-, 13- and 6-fold more potent than IFN-con1, in the HeLa, Huh7 and WISH antiviral assays, respectively. Likewise, B9X25 displayed significant improvements in potency being 17-, 11- and 8-fold more potent than IFN-con1 in the same three antiviral assays. The improved potency of B9X14 and B9X25 over IFN-con1 and IFN-α2b in the HeLa and Huh7-based EMCV antiviral assays is also observed under varying assay conditions, e.g., cell density, IFN treatment time, and multiplicity of infection (moi) (data not shown). B9X14 and B9X25 have Hill slopes that are steeper than both IFN-con1 and IFN-α2a in the Huh-7 and HeLa antiviral assays (SI Tables 3 and 5). This is reminiscent of IFN-β where the steeper Hill slope is believed to

Fig. 1. Genealogies of shuffled IFN B9.1.1 and B9.1.2. (*A*) Graphic representation of the genealogies of evolved IFNs B9.1.1 and B9.1.2 and the wild type IFNs from which they are derived. The gene segments are colored according to the parental gene from which they were derived. The vertical red bars in B9.1.1 represent the location of the pseudogene-derived amino acids. (*B*) Sequence alignment of B9.1.1 and B9.1.2 with IFN-α2a and IFN-con1.

Fig. 2. Antiviral activity of shuffled IFN-α compounds compared with IFN-con1, IFN-α2a, and IFN-α2b. (A) Graphic representation of the fold improvement of the 15 shuffled IFN-αs over IFN-con1 in the Huh7, WISH, and HeLa EMCV antiviral assays. The samples are listed in order of increasing potency in the Huh7 EMCV antiviral assay. Fold improvements were calculated as a ratio of mean EC$_{50}$ (ng/ml) values relative to IFN-con1 (SI Tables 3–5). (B) Exemplary dose-response curve for B9X14 and B9X25 compared with IFN-con1 and IFN-α2a in the HeLa EMCV antiviral assay. The calculated EC$_{50}$ value in this experiment for B9X25 is 0.00164 ng/ml, for B9X14 is 0.00314 ng/ml, for IFN-con1 is 0.133 ng/ml and for IFN-α2a is 0.415 ng/ml (mean ± SEM, n = 3).

be due to the higher affinity of IFN-β for IFNAR1 relative to IFN-α2 (12).

Although all members of the B9X series are significantly more potent than IFN-α2a and IFN-con1 in all three of these antiviral assays, the rank order of potencies among the B9X series varies suggesting that there may be significant differences in signaling by these hybrid IFN-α molecules in these three human cell lines (SI Tables 3–5). B9X14 and B9X25 have a broad spectrum of antiviral properties, exhibiting increased potency over IFN-con1 and IFN-α2b against primary isolates of HIV (SI Fig. 8), vesicular stomatitis virus and vaccinia virus (E. Fish and J. Kumaran, unpublished data). B9X14 and B9X25 are also potent antiviral agents against flaviviruses, protecting VERO cells from either West Nile virus- or yellow fever virus-induced cytopathic effect (Southern Research Institute, unpublished data).

Subsequently, the B9X series were assayed quantitatively in an assay in which differentiation of Th0 to Th1 cells was quantified by measuring the amount of IFN-γ secreted into the culture medium following treatment of naïve CD4$^+$ Th0 cells with an anti-CD3 antibody and a dose-response of the IFN-α samples (13, 19). All IFN-αs were tested in assays, using a minimum of four independent donors. Exemplary dose-response curves from the Th1 assay comparing B9X25 and B9X14 with IFN-con1 and IFN-α2a are shown in Fig. 3. The results demonstrate that all shuffled IFN-α com-

pounds examined were more potent than IFN-α2a in the Th1 differentiation assay, and 10 of the 13 shuffled IFN-α molecules tested are more potent than IFN-con1 (SI Table 6). B9X16, the most potent IFN tested in the Th1 induction assay, is 42-fold more potent than IFN-α2a and 15-fold more potent than IFN-con1 (SI Table 6). The Th1 inducing activity of B9X16 is fully blocked by a polyclonal antibody against human IFN-α confirming the specificity of this assay (SI Fig. 9)

IFN-α inhibits proliferation of many cell types, including haematopoietic progenitors (14). This antiproliferative activity of IFN-α induces dose limiting neutropenia and thrombocytopenia when these drugs are used therapeutically (5). Daudi is a human-derived Epstein–Barr virus-transformed B cell line that is highly IFN-α sensitive and serves as our surrogate assay for the antiproliferative effects on hematopoietic cell types (15). The antiproliferative activities of the shuffled IFN-α molecules in the B9X series and the commercial controls IFN-con1 and IFN-α2b were assessed in a tritiated thymidine uptake assay. As shown in Table 1, all of the shuffled IFNs tested displayed significantly reduced antiproliferative activity compared with that of IFN-con1 and IFN-α2b. Remarkably, the ratios of antiviral:antiproliferative potency in the B9X series range from 6- to 75-fold higher than IFN-con1 and the ratios of Th1:antiproliferative potency range from 3- to 81-fold higher than IFN-con1 (SI Table 7). In contrast to the Huh-7 and HeLa EMCV assays, the Hill slopes for B9X14 and B9X25 are not significantly steeper than that of IFN-α2a or IFN-con1 in the Daudi antiproliferation assay (Table 1).

Binding Properties of B9X14 and B9X25. The large increases in the ratios of antiviral:antiproliferative and Th1 inducing:antiproliferative activity relative to IFN-con1 and IFN-α2a raise the question of whether the affinity of these IFNs for the IFNAR1:IFNAR2 complex on Daudi cells is decreased or whether the complex signals less efficiently. A whole cell competition-binding assay was developed to investigate the relative binding affinity of selected IFN-α variants to the IFN-α receptor expressed on Daudi cells. Daudi is a nonadherent cell line with high cell surface expression of the type 1 IFN receptor making it suitable for directly assaying the affinity of IFNs for receptor expressed on whole cells. The assay used a flow cytometry-based detection of binding of biotinylated IFN-α (B9X14) to the Daudi IFN receptor. In direct saturation-binding experiments, biotinylated B9X14 displayed high affinity binding (50 − 100 pM) to Daudi cells (data not shown). The binding of the biotinylated B9X14 to the Daudi IFN-α receptor was specific as it could be completely blocked by preincubation of the Daudi cells with either excess unlabeled B9X14 or with an IFNAR-2 neutralizing antibody (SI Fig. 10). Apparent affinities of test IFNs for the IFN receptor were derived by measuring the concentration of unlabeled IFN-α variants (competitor) that reduced the binding of a biotinylated B9X14 (tracer) by 50%. B9X14 and B9X25 display 100-fold and 9-fold increased apparent affinity, respectively, compared with IFN-con1 (Table 2). The relative rank order in binding affinity among the shuffled IFN-αs and the reference IFNs is: B9X14 > B9X25 > B9.1.2 > IFN-con1 ≥ IFN-α2a > IFN-α8 ≫ IFN- α1.

Discussion

In this study, we report IFN-α molecules wherein we have modified three major classes of IFN-mediated activities to yield evolved variants that exhibit an increase in both absolute antiviral and Th1 activities and in the ratios of antiviral: antiproliferative and Th1: antiproliferative activity. B9X14, for example, exhibits a 32-fold increase in antiviral:antiproliferative potency and a 16-fold increase in Th1 inducing:antiproliferative potency relative to IFN-con1 (SI Table 7). Remarkably, B9X14 exhibits a 96-fold increased affinity, relative to IFN-con1, for the IFNAR1:IFNAR2 complex expressed on Daudi cells, and yet exhibits significantly lower antiproliferative activity on this cell line.
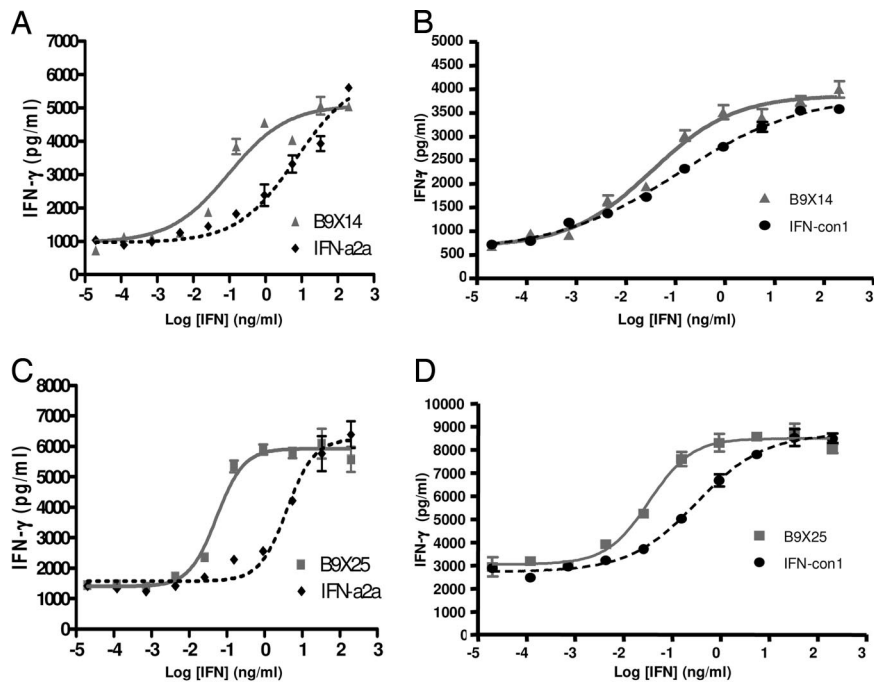
Fig. 3. Th1-inducing activity of shuffled IFN-α compounds compared with IFN-con1 and IFN-α2a. Exemplary dose-response curves are shown as follows: (*A*) B9X14 and IFN-α2a, EC_{50} = 0.096 and 6.95 ng/ml, respectively; (*B*) B9X14 and IFN-con1, EC_{50} = 0.10 and 0.82 ng/ml, respectively; (*C*) B9X25 and IFN-α2a, EC_{50} = 0.053 and 3.94 ng/ml, respectively; (*D*) B9X25 and IFN-con1, EC_{50} = 0.033 and 0.305 ng/ml, respectively. The pair of curves in each panel is from triplicate samples of each IFN run in a single plate to minimize between-plate variance (mean ± SEM, n = 4). The EC50s were calculated as described in SI Table 6. We tested these four variants in 8–12 independent donors, and in all cases, both B9X14 and B9X25 were significantly more potent than both IFN-α2a and IFN-con1 (SI Table 6).

Pseudogene-Derived Sequences Contribute Significantly to the Novel Phenotype. The seven pseudogene-derived residues in B9.1.1 were broken into three motifs and these motifs were permuted with the corresponding sequences in B9.1.2 to enable us to assess whether any of these motifs contributed to the activity profile of interest in multiple sequence contexts (SI Fig. 7). As indicated in Fig. 4*A*, the presence of pseudogene derived M2 correlates with high ratios of both antiviral:antiproliferative and Th1:antiproliferative potency. The four residues comprising M2 are not present in any functional member of the IFN-α family (SI Fig. 6) but interestingly F57/Y58 are present at the homologous position in IFN-κ (1). This motif occurs outside of the known IFNAR2 binding site but within the presumptive IFNAR1 binding site (ref 12; Fig. 4*C*), suggesting that they may play a role in forming a complex with IFNAR1.

Implications for Models of the IFN-α:IFNAR1:IFNAR2 Ternary Complex. Roisman *et al.* (12) have recently mapped the IFN-α2:IFNAR1 binding site by alanine scanning. They showed that among IFN-β and a series of IFN-α2 alanine point mutants that vary over three orders of magnitude in potency, the affinity for IFNAR1 correlates well with antiproliferative activity but that antiviral potency seems to hit a plateau such that IFN-β has 30-fold higher affinity for IFNAR1, 45-fold higher antiproliferative activity (WISH) and twofold higher antiviral activity (WISH VSV). Interesting, Rois-

man *et al.* report a positive correlation between the Hill slope of the antiviral dose-response curves and affinity for IFNAR1. Our observations that B9X14 and B9X25 have (*i*) higher antiviral and Th1-inducing activities, (*ii*) higher affinities for the IFNAR1:IFNAR2 receptor expressed on Daudi cells, and (*iii*) steeper Hill slopes than IFN-con1 and IFN-α2a in the Huh-7 EMCV and HeLa EMCV antiviral assays (SI Tables 3 and 5) are consistent with a model wherein the affinities of these IFN-α molecules for IFNAR1 is increased.

However, the trend in functional activity is very different from that seen by Roisman *et al.* (12) and Jaitin *et al.* (16) who see correlated increases in both antiviral and antiproliferative activity with increasing affinity. In contrast, we report IFN-α molecules with increased affinities for the IFN receptor complex, increased antiviral activity, increased Th1-inducing activity but decreased antiproliferative activity. Four novel contiguous pseudogene-derived residues in the B9X series correlate with these unusual ratios (Fig. 4). Roisman and others have suggested that differences in binding to IFNAR1 may underlie the striking differences between type I IFNs in cellular activities. Indeed, the high ratio of antiviral to antiproliferative activity exhibited by the B9X series is reminiscent of limitin, a recently discovered member of the type I IFN family with a similar activity profile (17). Given that B9X14 and B9X25 differ by >20 aa from human IFN-α2 and IFN-con1, that they were derived by explicit selection and subsequent recombination to optimize the rare phenotype of interest, and that the activity ratios are correlated with a novel pseudogene-derived motif in the IFNAR1 binding site, we suggest that these gene-shuffled IFN-α molecules may form a ternary complex with IFNAR1/2 that signals substantially differently than that of IFN-con1 or IFN-α2. Illumination of the mechanistic basis of this phenomenon will advance our understanding how type I IFNs mediate such remarkably pleiotropic effects on diverse cell lines.

Clinical Implications. Mathematical modeling of the viral decline of HCV during standard IFN-α treatment suggests that the rate of viral decline in the first 24 h ("early" viral kinetics) is believed to be due to the direct antiviral activity of IFN-α on naïve and infected cells. The slower rate of decline in viral load observed during the late phase of viral clearance is believed to be due to the antiviral

Table 2. Summary of the relative affinities of the wild type, shuffled and control interferons in the Daudi binding affinity assay

Description	IC_{50}, nM	SD	n	Fold over IFN-con1
B9X14	0.04	0.01	13	96.6
B9X25	0.44	0.09	6	9.05
B9.1.2	2.04	0.61	5	1.95
IFN-con1	3.97	1.19	15	1
IFN-α2a	4.62	0.82	11	0.86
IFN-α8	7.45	0.57	3	0.53
IFN-α1	1450	422	3	0.003

Fold improvements were calculated as a ratio of the mean IC_{50} (nM) values relative to IFN-con1.
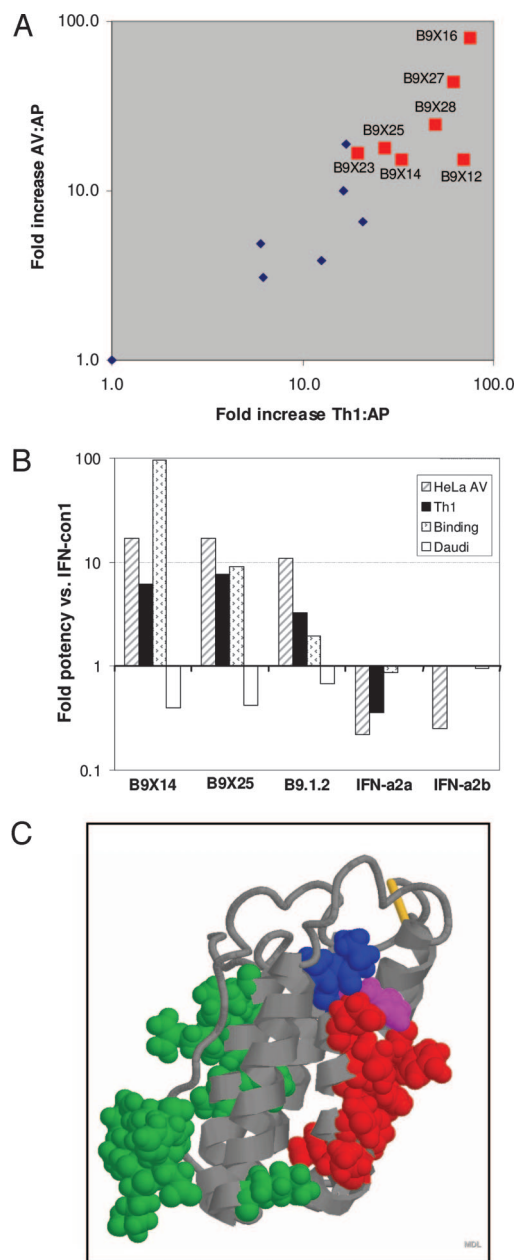
Fig. 4. The presence of pseudogene motif 2 is highly correlated with high ratio of antiproliferative:antiviral and antiproliferative:Th1 inducing activity. (*A*) The ratios of calculated antiviral:antiproliferative and Th1:antiproliferative potencies (SI Table 7) are plotted. Red squares correspond to variants containing pseudogene motif 2 (FLFY), and blue diamonds correspond to variants containing motif 2 from B9.1.2. (*B*) Summary of the fold potency of B9X14, B9X25, B9.1.2, IFN-α2a, and IFN-α2b versus IFN-con1 in the HeLa EMCV antiviral assay (striped bars), the Th1 differentiation assay (black bars), the Daudi binding assay (stippled bars) and the Daudi antiproliferation assay (open bars). (*C*). IFNAR1 (red) and IFNAR2 (green) binding sites are displayed on the coordinates of IFN-α2 (Protein Data Bank accession no. 1997-12-03). Residues corresponding to the pseudogene derived motif 2 (Phe-Leu-Phe; residues 54–56) are shown in blue, and residue Y57, which arose by a mutation C>T in the H57 codon of IFN-α4, is shown in mauve.

activity and an increase in the infected cell death rate (18). It has been demonstrated that a successful response to antiviral therapy is associated with the development of Th1 type immune responses to a broad range of HCV T cell epitopes, supporting the view that induction of Th1 differentiation by IFN-α may play an important

role in the treatment of HCV (7, 8). The gene-shuffled IFN-α molecules described here with unprecedented ratios of antiviral:antiproliferative and Th1:antiproliferative activity hold significant promise for providing clinicians with novel IFNs with a significantly improved therapeutic index for treatment of chronic viral diseases, such as chronic hepatitis C. It is interesting to note that 50 years after the first description of the type I IFNs, new insights into their mode of action are being unveiled and novel therapeutics based on this prototypical cytokine are likely to be developed in the coming years.

Materials and Methods

Library Construction. Construction of the gene-shuffled IFN libraries was performed as described in ref. 9. In this study, these libraries were PCR amplified and cloned into pcDNA3.1 to enable CHO expression.

IFN Reagents. Commercial preparations of consensus IFN (INFERGEN; InterMune, Brisbane, CA), IFN-α2a (ROFERON; Roche, Nutley, NJ) and IFN-α2b (INTRON A; Schering Plough, Kenilworth, NJ) were used as controls throughout this study.

CHO expression and purification of shuffled IFN-α's. IFN-α genes were cloned into a CHO expression vector (pcDNA3.1-derived) containing an IFN-α6 leader sequence and an E-tag followed by a His-tag fused to the C terminus of the IFN-α sequence. In this construct, IFN-α expression is driven by the CMV promoter. CHO-K1 cells (ATCC, CCL-61) stable transfectants were selected in the presence of G418 and further subcloned by single cell sorting, using flow cytometry. High expressing subclones were identified by Western/dot blot analysis, using anti-IFN α and anti-E tag antibodies and expanded into roller bottles containing CHO III A medium (Invitrogen, Carlsbad, CA). The shuffled IFN-α molecules were purified from harvested roller bottle media by anti-E tag affinity purification, using the RPAS kit (GE Healthcare, Little Chalfont, U.K.). The purified shuffled IFN-α's were quantified with the BCA assay kit (Pierce) and further characterized by SDS/PAGE analysis for purity estimation and MALDI-TOF for molecular mass verification. The high-throughput Th1 and Daudi antiproliferation assays were performed on transient CHO transfection supernatants. Expression levels were determined by quantitative Western blot analysis, using anti-E tag antibodies.

B9X14 was biotinylated on primary amines, using biotin-NHS (Pierce Chemical, Rockford, IL) according to the manufacturer's instructions. Biotinylation of B9X14 did not affect the biological activity of the molecule as determined in an antiviral activity assay (data not shown).

Antiviral Assays. Antiviral activity of the B9X series was determined by a cytopathic effect bioassay that measures the ability of IFN preparations to protect human cell lines from cytotoxicity due to infection with EMCV essentially as described in ref. 11. For the Huh7 EMCV antiviral assay, 6×10^4 Huh7 cells were plated into 96-well flat-bottom microtiter plates and allowed to recover for 4 h at 37°C before incubation with an eight-point, threefold serial dilution of the IFN-α samples in triplicate. After 16 h of IFN treatment, the IFN samples were removed, and the cells were challenged with EMCV (ATCC, VR-129B) at an moi of 0.034 (moi based relative to initial seeding density) for 24 h. Inhibition of cytopathic effect by the IFN was determined by tetrazolium salt metabolism assay, WST1 (Roche Applied Sciences, Indianapolis, IN). The WISH EMCV assay was performed essentially the same, except that the initial seeding density was 3×10^4 WISH cells (ATCC, CCL-25) per well and the viral infection was performed at an moi of 5. In the HeLa EMCV assay, the HeLa cells (ATCC, CCL-2) were plated at a density of 1×10^4 cells/well and allowed to recover for 24 h before treatment with the IFN samples (eight-point, fivefold serial dilution) and EMCV infection (moi of 5).

Percent antiviral protection was calculated from the optical density and defined as the percent of surviving cells in wells treated with virus and IFN relative to wells treated with IFN alone. Three replicate dose-response curves per microtiter plate were used to derive one log EC_{50} estimate using a four-parameter logistic equation (sigmoidal) curve fit (GraphPad Prism 4.00; GraphPad Software, San Diego, CA). For many of the IFN proteins, potency estimates were based on both replicate independent experiments and replicate protein batches.

To test the antiviral activity of B9X14 and B9X25 against HIV-1, primary $CD4^+$ T cells were purified from human peripheral blood mononuclear cells and infected with a primary stock of a dual-tropic HIV-1 isolate (HIV-1_{SF2}; a multiplicity of infection of 0.01). The infected $CD4^+$ cells were then cultured for 10 days in complete RPMI medium 1640 supplemented with IL-2 (100 units/ml) in the presence or absence of a fivefold IFN dilution series. Viral replication was monitored by measuring the concentration of p24 antigen in the cell culture fluids, using an ELISA at days 4, 7, and 10 after infection (Beckman Coulter, Fullerton, CA).

Daudi Tritiated Thymidine Uptake Assay. The antiproliferative activity of IFN was determined by using a standard proliferation assay (15). Daudi cells (ATCC, CCL-213) plated at 10,000 cells per well were incubated with a 12-point, fourfold serial dilution of the various IFNs. After 48 h, 1μCi of methyl-^{3}H-thymidine [Amersham Pharmacia (Little Chalfont, U.K.); catalog no. TRK758] was added to each well followed by incubation for 24 h. The cells were harvested on the following day onto filter paper by a cell harvester (Tomtec, Hamden, CT), and ^{3}H-thymidine incorporation was measured by using a scintillation counter (MicroBeta; Wallac Oy, Turku, Finland). Counts per minute were plotted against the log of the IFN concentration. Four replicate dose-response curves per microtiter plate were used to derive one EC_{50} estimate.

Th1 Induction Assay. The Th1 assay was designed to monitor the enhancement of differentiation of human naïve T cells into Th1 cells by IFN-α as determined by the amount of IFN-γ secreted into the culture supernatant. The Th1 assay is a modified version of a previously published assay (19) and is described briefly below. Human peripheral blood mononuclear cells were isolated from buffy coats (Stanford Blood Center, Stanford, CA) by centrifugation through a Histopaque/Ficoll gradient (Sigma, St. Louis, MO). Platelets were removed by centrifugation following a PBS wash, and red blood cells were lysed by using a standard red blood cell lysis buffer. Naïve T cells were separated from the total peripheral blood mononuclear cells population by antibody staining and cell sorting ($CD45RA^+$, $CD4^+$, $CD8^-$, $CD14^-$, $CD20^-$). A modular flow cytometer was used to FACS sort and seed 10,000 cells per well into 96-well round bottom culture plates. The naïve T cells were activated by the addition of CD3/CD28 T cell expander Dynabeads (DynalBiotech, Lake Success, NY) and treated with a 10-point, sixfold serial dilution of each IFN in triplicate for 6 days at 37°C in a humidified 5% CO_2 incubator. Supernatants from each well were

harvested and the concentration of IFNγ released into the culture supernatant was determined by using a commercial ELISA kit (R&D Systems, Minneapolis, MN). We found that the percentage of Th0 cells correlated with donor variability. Donors with <15% Th0 cells tended to have a high percentage of Th1 cells, high background levels of IFN-γ in the PBS controls, and unusually wide 95% confidence intervals for the estimation of the EC50s. We therefore rejected buffy coats with <15% Th0 cells and selected among the four donors on any given day for the two buffy coats with the highest percentage of Th0 cells. The high-throughput Th1 assay was conducted essentially as described above with the exception being that the IFN samples were tested as two duplicate sixfold dilutions. Three replicate dose-response curves per microtiter plate were used to derive on EC_{50} estimate.

Binding Affinity of B9X14 and B9X25. The direct saturation-binding affinity of B9X14 was determined essentially as follows. Serially diluted biotinylated B9X14 (0–750 pM) was incubated for 4 h at 4°C with Daudi cells in either the absence or the presence of unlabeled B9X14. In some instances, the Daudi cells were preincubated with a neutralizing antibody against IFNAR-2 (Caltag Laboratories, Burlingame, CA). Bound biotinylated B9X14 was then detected by flow cytometry after staining with SA-PE (Dako, Carpinteria, CA). All steps were performed in 96-well microtiter plates. The affinity (K_d) of biotinylated B9X14 was determined as the concentration of biotinylated B9X14 yielding half maximum binding at equilibrium.

In the competition binding assays, Daudi cells were incubated in 96-well plates with a concentration of biotinylated B9X14 close to its affinity constant (50 pM) in the presence of increasing concentrations of unlabeled shuffled IFNs (B9X14, B9X25, B91.2), wild type IFN subtypes (IFN-α1, IFN-α8), or commercially produced IFNs (IFN-con1, IFN-α2a) as competitive ligands. The residual binding of the tracer (biotinylated B9X14) was then detected by flow cytometry after staining the cells with SA-PE. The concentration of competitor that reduced the tracer binding by 50% (IC_{50}) was reported as a measure of relative affinity.

Statistical Analysis. Significant differences between the shuffled IFNs and the control molecules in the Huh7 EMCV, HeLa EMCV, Th1 differentiation, and Daudi assays was determined by using a two-way ANOVA with a Fisher's least significant difference post hoc test with log-transformed EC_{50} data. The Levene's, Hartley F-max, Cochran C, and Bartlett chi square tests for the homogeneity of variances was performed on all data sets. As the data set for the WISH EMCV antiviral assay failed to pass the above-mentioned assumption tests, significant differences were determined with a two-sample t test. The statistical software package Statistica, Version 7 (StatSoft, Tulsa, OK) was used for all statistical analyses.

1. Pestka S, Krause CD, Walter MR (2004) *Immunol Rev* 202:8–32.
2. Foster GR, Masri SH, David R, Jones M, Datta A, Lombardi G, Runkell L, deDios C, Sizing E, James MJ, Barelli-Berg FM (2004) *J Immunol* 173:1663–1670.
3. Hibbert L, Foster GR (1999) *J Interferon Cytokine Res* 19:309–318.
4. Kurtzman AL, Govindarajan S, Vahle K, Jones JT, Heinrichs V, Patten PA (2001) *Curr Opin Biotechnol* 12:361–370.
5. Kowdley KV (2005) *J Clin Gastroenterol* 39:S3–S8.
6. Maloy KJ, Burkhart C, Junt TM, Odermatt G, Oxenius A, Piali G, Zinkernagel RM, Hengartner H (2000) *J Exp Med* 191:2159–2170.
7. Cramp ME, Rossol S, Chokshi S, Carucci P, Williams R, Naoumov NV (2000) *Gastroenterology* 118:346–355.
8. Kamal SM, Fehr J, Roesler B, Peters T, Rasenack JW (2002) *Gastroenterology* 123:1070–1083.
9. Chang CC, Chen TT, Cox BW, Dawes GN, Stemmer WP, Punnonen J, Patten PA (1999) *Nat Biotechnol* 17:793–797.
10. Goeddel DV, Leung DW, Dull TJ, Gross M, Lawn RM, McCandliss R, Seeburg PH, Ullrich A, Yelverton E, Gray PW (1981) *Nature* 290:20–26.

11. Familletti PC, Rubinstein S, Pestka S (1981) in *Methods in Enzymol*, Vol 78, ed Pestka S (Harcourt, NY), pp 387–94.
12. Roisman LC, Jaitin DA, Baker DP, Schreiber G (2005) *J Mol Biol* 353:271–281.
13. Rogge L, D'Ambrosio D, Biffi M, Penna G, Minetti LJ, Presky DH, Adorini L, Sinigaglia F (1998) *J Immunol* 161:6567–6574.
14. Kato K, Kamezaki K, Shimoda K, Numata A, Haro T, Aoki K, Ishikawa F, Takase K, Ariyama H, Matsuda T, *et al.* (2003) *Br J Haematol* 123:528–535.
15. Scarozza AM, Collins TJ, Evans SS (1992) *J Interferon Res* 12:35–42.
16. Jaitin D, Roisman LC, Jaks E, Gavutis M, Piehler J, Van der Heyden J, Uze G, Schreiber G (2006) *Mol Cell Biol* 26:1888–1897.
17. Kawamoto S, Oritani K, Asakura E, Ishikawa J, Koyama M, Miyano K, Iwamoto M, Yasuda S, Nakakubo H, Hirayama F, *et al.* (2004) *Exp Hematol* 32:797–805.
18. Neumann AU, Lam NP, Dahari H, Gretch DR, Wiley TE, Layden TJ, Perelson AS (1998) *Science* 282:103–107.
19. Foster GR, Germain C, Jones M, Lechler RI, Lombardi G (2000) *Eur J Immunol* 30:3228–3235.